Experimental Research on Resonance Characteristics of a High-Efficiency Moving Coil Linear Compressor for J-T Throttle Refrigerator

J. Sun[1,2], J. Li[1], Y. Liu[1,2], Z. Huang[1,2], N. Wang[1], J. Cai[1,2]

[1]Key Laboratory of Technology on Space Energy Conversion, Technical Institute of Physics and Chemistry, Chinese Academy of Science, Beijing 100190, China
[2]University of Chinese Academy of Sciences, Beijing 100049, China

ABSTRACT

In order to study the mass flow rate, efficiency and dynamic response characteristics of a linear compressor for a J-T throttle refrigerator, an online test system was set up to monitor the important dynamic response parameters. The performance and dynamic response characteristics at different driving frequencies were tested under the conditions of fill pressure of 0.7 MPa, pressure ratio of 3 and stroke of 10 mm. At the resonant frequency (65 Hz), motor efficiency, volume efficiency, isentropic efficiency and isothermal efficiency have the maximum value, which are respectively 86.7%, 76.5%, 64.1% and 54.5%. A mass flow rate of 0.84 gr/s, and corresponding input power of 151 W. The current waveform has non-sinusoidal distortion, and its bimodal phenomenon on the positive half axis reveals the essential reason for high efficiency at resonance frequency. In addition, the nonlinear distortion law of current waveform can be used to quickly and visually judge whether the linear compressor is resonant in the experiment. In addition, piston offset, opening and closing of the discharge valve, and power loss during suction and discharge process were also studied. The study is very important to analyze the operating state of the linear compressor, judge the matching of the gas valve assembly and optimize the linear compressor.

INTRODUCTION

Because of the advantages of high efficiency, low vibration, stable operation and strong electromagnetic resistance, J-T throttling refrigerators have been successfully used in space such as: James Webb Space Telescope (NASA) [1-3], Astro-H and SPICA space exploration mission (JAXA/ESA/NASA)[4-6]. As the core component of the J-T throttling refrigerator, the efficiency of the linear compressor plays an important role in the total efficiency of the throttling refrigerator[7]. As we know, the linear compressor has the highest efficiency at resonance frequency, so the research on resonance characteristics of the linear compressor has always been a hot spot. Some work has been carried out to study the flow rate and efficiency characteristics of linear compressor at resonance and non-resonance[8]. Other work has been done to study how to accurately calculate the value of resonance frequency, such as the average gas force method and the gas force Fourier equivalent method[9-10]; and some work has been implemented to study the response characteristics of current, displacement and gas force at resonance frequency[11].

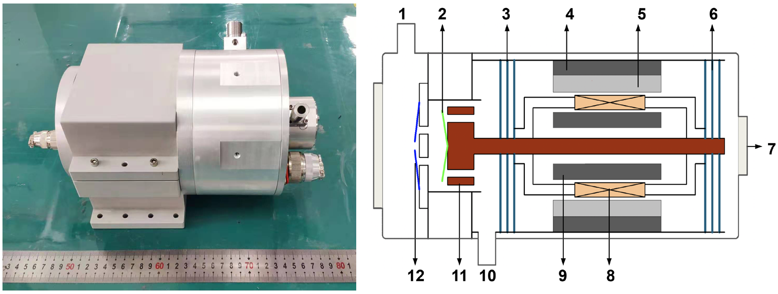

Figure 1. Schematic diagram of linear compressor structure. 1 discharge outlet, 2 suction valve, 3 flexure spring, 4 outer core, 5 permanent magnet, 6 flexure spring, 7 glass visualization window, 8 copper coil, 9 inner core, 10 suction inlet, 11 piston, 12 discharge valve.

However, the essential reason for the highest efficiency of the linear compressor is rarely studied. In addition, there is a lack of quick and visualized method to judge whether the linear compressor is in resonance state in the experiment. In order to solve the above two problems, an on-line test system for monitoring important dynamic parameters of the linear compressor was set up. The performance and dynamic response characteristics of the linear compressor at resonance and non-resonance frequencies under the conditions of fill pressure 0.7 MPa, pressure ratio 3 and stroke 10 mm were tested. The mass flow rate, efficiency, discharge valve lift, current, cylinder pressure, displacement, piston offset, discharge pressure, suction pressure and PV diagram were obtained. The dynamic responses of linear compressors with and without resonance were both analyzed.

EXPERIMENTAL APPARATUS

Figure 1 shows the structure diagram of the moving coil linear compressor. The dynamic components of the prototype are well supported on two sides by flexure springs to reduce the dry friction between the piston and the cylinder. The inner part of the piston is hollowed out as the suction channel to increase the suction capacity. The suction valve is a ring valve, and the discharge valve is composed of four small reed valves.

Figure 2 shows the schematic diagram of the linear compressor on-line monitoring system. The linear compressor is driven by sinusoidal voltage. The gas is compressed in the compressor, cooled in the high-pressure heat exchanger, expanded in the throttle valve, cooled in the low-pressure heat exchanger, and finally sucked into the compressor to complete the whole process. Two laser displacement sensors (X1 and X2) are installed to measure in real-time the discharge valve lift

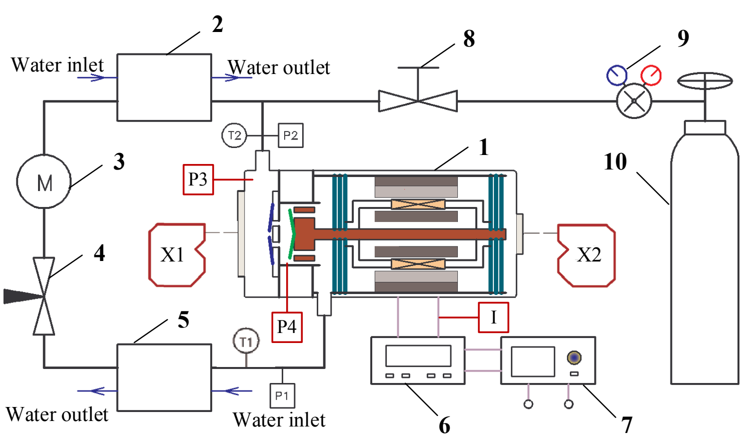

Figure 2. Schematic diagram of the linear compressor on-line monitoring system: 1 linear compressor, 2 high pressure heat exchanger, 3 mass flow meter, 4 manual throttle valve, 5 low pressure heat exchanger, 6 power meter, 7 NF power supply, 8 manual diaphragm valve, 9 gas reduction pressure valve, 10 nitrogen cylinder.

Table 1. The instrument list of the test system.

Instruments	Mode	Quantity	Information
Hall current clamp	LeCroy	1	Response frequency: 50MHz;
Laser displacement sensor	KEYENCE LK-H080	2	Resolution: 0.10μm
Dynamic high frequency Absolute pressure sensor	Kunshan Double Bridge CYG1401F	1	Uncertainty: 0.25%; Response frequency: 20kHz;
Miniature high frequency Absolute pressure sensor	Kunshan Double BridgeCYG1502AMLF	1	Uncertainty: 0.5%; Response frequency: 20kHz;
Thermometer	Four-wire platinum resistance	2	Accuracy: 0.1K
Pressure Transmitters	Beijing zhuochen	2	Accuracy: 0.5%
Coriolis Mass flowmeter	Beijing Sincerity	1	Accuracy: 0.2%
Power meter	Hangzhou Yuanfang PF9811	1	Accuracy: 0.5%

and piston displacement. Two dynamic pressure sensors (P3 and P4) are installed to measure the real-time pressure in the discharge chamber and the cylinder respectively. A Hall current clamp is fixed on the compressor power line to measure the real-time current waveform. These high frequency signals are transmitted to an oscilloscope for display, analysis and storage. Two pressure transmitters (P1 and P2) are used to measure suction and discharge pressure of the linear compressor respectively. Two, four wire PT100 thermal resistance thermometers (T1 and T2) are used to measure suction temperature and discharge temperature. A Coriolis mass flowmeter is used to measure the mass flow rate. These parameters are collected, displayed and stored by LabVIEW software on a computer through NI acquisition card.

The instrument list of the test system is shown in Table 1.

RESULTS AND DISCUSSIONS

The prototype is tested to study the flow rate, efficiency and dynamic response characteristics at resonance frequency and non-resonance frequency. The working fluid is N_2, the fill pressure is 0.7 MPa, the suction pressure is 0.285 MPa, the pressure ratio is 3, the fixed piston stroke is 10 mm, and the frequency range is from 55 Hz to 67.5 Hz.

The Mass Flow rate and Efficiency

The motor efficiency can be calculated by Equation 1:

$$\eta_{motor} = 1 - \frac{I_{rms}^2 R}{\dot{W}_{in}} \tag{1}$$

where I_{rms} is the drive current, R is the resistance of the copper coil, and $\dot{W}_{in}$ is the input power. The volumetric efficiency of the linear compressor can be obtained by Equation 2:

$$\eta_v = \frac{\dot{m}_0}{\dot{m}_{theory}} = \frac{4\dot{m}_0 R_g T_1}{\pi D^2 S f P_1} \tag{2}$$

where D is the piston diameter, S is the piston stroke, and f is the drive frequency, $\dot{m}_0$ is the system mass flow, R_g ratio of isobaric to isochoric specific heats and T_1 is the compressor suction temperature.

The isentropic efficiency and isothermal efficiency of the linear compressor are obtained by equation 3 and equation 4:

$$\eta_{isen} = \frac{\dot{W}_{isen}}{\dot{W}_{in}} = \frac{k}{k-1}\dot{m}_0 R_g T_1 \left[\left(\frac{P_2}{P_1} \right)^{\frac{k-1}{k}} - 1 \right] / \dot{W}_{in} \tag{3}$$

$$\eta_{iso} = \frac{\dot{W}_{iso}}{\dot{W}_{in}} = \dot{m}_0 R_g T_1 \ln\left(\frac{P_2}{P_1} \right) / \dot{W}_{in} \tag{4}$$

where k is the isentropic coefficient (k=1.4 for N_2) is 1.4, P_2 is the discharge pressure, P_1 is the suction pressure.

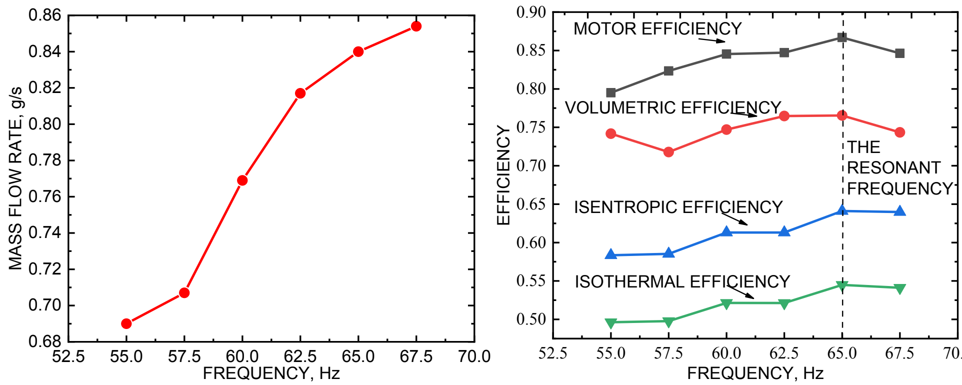

Figure 3. Mass flow rate and efficiency at different frequencies.

Figure 3 shows the mass flow rate and efficiency at different frequencies. With the increase of frequency, the mass flow rate always increases, but the gradient of increase decreases. Motor efficiency, volume efficiency, isentropic efficiency and isothermal efficiency all increase first and then decrease with the increase of frequency. Motor efficiency, volume efficiency, isentropic efficiency and isothermal efficiency has the maximum value at the frequency of 65 Hz, which respectively is 86.7%, 76.5%, 64.1% and 54.5%. At this time, mass flow rate is 0.84 gr/s, and corresponding input power is 151 W. It is easy to judge that the resonance frequency under this operating condition is 65 Hz.

Discharge Valve Lift

Figure 4 shows discharge valve lift at different frequencies. It can be seen that the peak displacement of the discharge valve and the opening time of discharge valve increase all the time with the increase of frequency. When the discharge valve is closed, it collides with the valve plate and bounces. As the frequency increases, the height of the rebound increases. The lift of the discharge valve increases approximately linearly with the increase of frequency. This is because with the increase in frequency, the average gas velocity (average Ma number) between the discharge valve and the valve plate increases, and the gas pressure difference on both sides of the discharge valve plate increases, so the lift of the valve plate increases and the rebound displacement also increases.

Displacement and Piston Offset

Figure 5 shows piston displacement and piston offset at different frequencies. The displacement waveform of the linear compressor is almost sinusoidal. The piston of the linear compressor will offset to the direction of the motor, and the piston offset value will decrease approximately

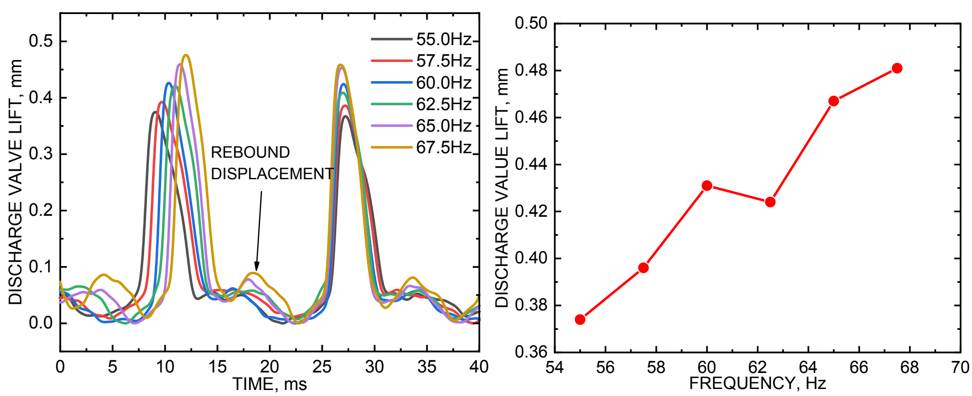

Figure 4. Discharge valve lift at different frequencies.

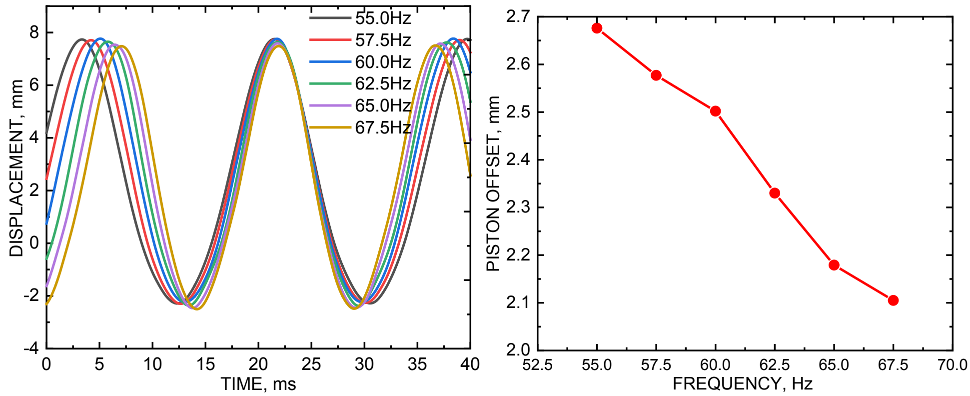

Figure 5. Piston displacement and piston offset at different frequencies.

linearly with the increase of frequency. This is because with the increase of frequency, the average gas force in the cylinder decreases, the gas pressure difference between the two sides of the piston decreases, and the piston offset decreases.

The Current Waveform

Figure 6 shows current waveform at different frequencies. The non-linear distortion of the current waveform occurs in the positive half of the waveform. With the increase of frequency, there are two peaks in the positive half, in which the peak on the left side increases all the time and the peak on the right side decreases all the time. The two peaks on the positive half of the current waveform obtain the same shape and size at resonance frequency. The unique current waveform distortion can be used to determine whether the linear compressor operates at resonance frequency, which avoids complicated calculation and is very visualized. With the increase of frequency, the current in a single cycle first increases and then decreases, and there is a minimum value of 0.07 A/Hz at resonance frequency (65 Hz), which is highly related to the current non-linear distortion. This shows that the serious non sinusoidal distortion of the resonant current is the essential reason for the minimum driving current and the highest motor efficiency for linear compressor.

P-V diagram

Figure 7 shows the P-V diagram at 55Hz/60Hz/65Hz. The PV work (i.e. the total area of PV diagram) of linear compressor increases in a period with an increasing frequency. The working process of linear compressor includes compression process (1-2), discharge process (2-3), expansion process

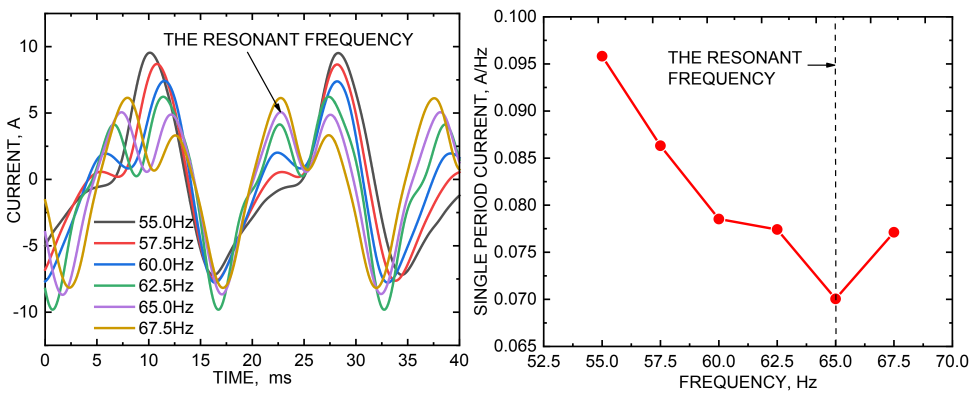

Figure 6. Current waveform at different frequencies.

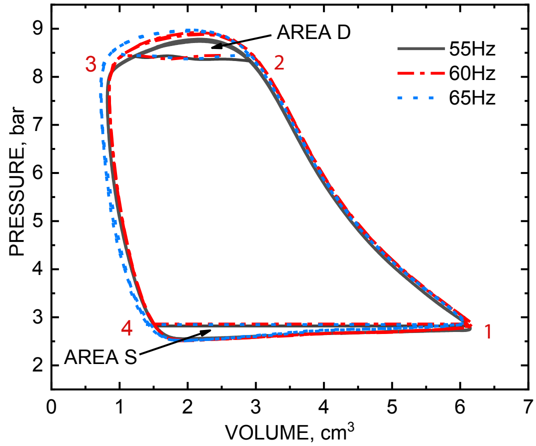

Figure 7. the P-V diagram at 55Hz/60Hz/65Hz.

(3-4) and suction process (4-1). It can be seen that the variable coefficient of compression process (i.e. gradient of curve 1-2) and expansion process (i.e. gradient of curve 3-4) are invariant at different frequencies, the areas of S and D correspond to the work loss of suction and discharge process respectively. It can be seen that the work loss of suction process almost remains constant, but the work loss of discharge process increases with the increase of frequency.

Dynamic Analysis

Figure 8 shows the cylinder pressure, discharge pressure, suction pressure, discharge valve lift, piston displacement and current at non-resonant frequencies and resonant frequency. According to the relationship between cylinder pressure, suction pressure and discharge pressure, four working processes of the linear compressor can be obtained: expansion process (3-4), suction process (4-1), compression process (1-2) and discharge process (2-3). The non-sinusoidal current deformation mainly occurs in the compression process and the discharge process. Compared with the current waveform under non-resonant frequencies, the current waveform under resonance frequency has two equal peaks in the compression process and discharge process, and the current value in positive half is far less than that under non-resonant frequencies. This is the fundamental reason why the single cycle current is the minimum and the motor efficiency is the highest when the linear compressor operates at resonance frequency. By observing the opening and closing time of the discharge valve, it can be seen that the discharge valve can be opened and closed on time without delay at 55 Hz, however, the discharge valve can only be opened accurately without delay but is closed with delay at 65 Hz. This phenomenon is very important for the valve design of high frequency linear compressor.

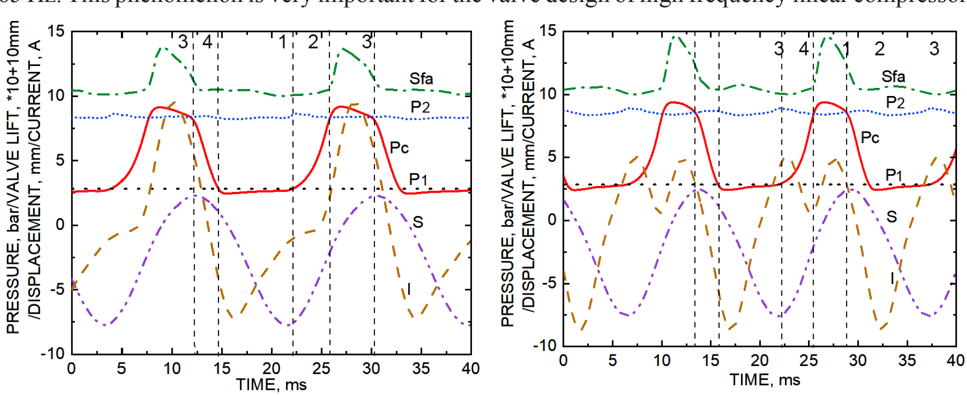

Figure 8. Cylinder pressure (Pc), discharge pressure (P2), suction pressure (P1), discharge valve lift (Sfa), piston displacement (S), current at non-resonant and resonant frequencies (I).

CONCLUSION

The resonant frequency is 65 Hz under the condition of fill pressure of 0.7 MPa, pressure ratio of 3 and stroke of 10 mm. At the resonant frequency, motor efficiency, volume efficiency, isentropic efficiency and isothermal efficiency has the maximum value, which is 86.7%, 76.5%, 64.1% and 54.5% respectively. With a mass flow rate of 0.84 gr/s, and corresponding input power is 151 W.

The non-sinusoidal current deformation mainly occurs in the compression process and the discharge process. Compared with the current waveform under non-resonant frequency, the current waveform under resonance frequency has two equal peaks in the compression process and discharge process, and the current value in the positive half is far less than that under non-resonant frequencies. This is the fundamental reason why the single cycle current is the minimum and the motor efficiency is the highest when the linear compressor operates at resonant frequency.

With the increase of frequency, the lift of discharge valve increases, the delay of discharge valve closing time increases, and the work loss of discharge process increases.

ACKNOWLEDGMENT

Supported by the National Natural Science Foundation of China (Grant No. 51776213) and the Strategic Priority Research Program of Chinese Academy of Sciences. (Grant No. XDA18000000, No. XDA18040000).

REFERENCES

1. Levenduski, R., Gully, W., Lester, J., “Hybrid 10 K Cryocooler for Space Applications,” *Cryocoolers 10,* Plenum Publishing Corp., New York (1999), pp.505-511.

2. Lindensmith, C. A., Bowman, R. C., Wade, L. A., et al., “Cryocooler Options for NGST and other Space Applications,” *Next Generation Space Telescope Science and Technology*, (2000).

3. DiPirro, M., Johnson, D. L., Shirron, P., “Cryogenic Technology for CMBPol,” *Journal of Physics: Conference Series*, IOP Publishing, Vol. 155, No. 1 (2009), p. 012008.

4. Sugita, H., Sato, Y., Nakagawa, T., et al, “Development of Mechanical Cryocoolers for the Japanese IR Space Telescope SPICA,” *Cryogenics*, Vol. 48, No. 5 (2008), pp. 258-266.

5. Sugita, H., Sato, Y., Nakagawa, T., et al., “Cryogenic System Design of the Next Generation Infrared Space Telescope SPICA,” *Cryogenics*, Vol. 50, No. 9 (2010), pp. 566-571.

6. Shinozaki, K., Sugita, H., Sato, Y., et al., “Developments of 1~4 K Class Space Mechanical Coolers for New Generation Satellite Missions in JAXA,” *Journal of Physical Chemistry B*, Vol. 112, No. 15 (2008), p. 4561.

7. Ma, Y. X., "Study on Multi-stage Throttling Process Driven by Three-stage Linear compressor in Space Liquid Helium Temperature Region," Chinese Academy of Sciences (2017).

8. Liang, K., "A Novel Linear Electromagnetic-drive Oil-free Refrigeration Compressor," University of Oxford (2014).

9. Zou, H. M. , Li, C., Tang, M.S., et al., “Online measuring method and dynamic characteristics of gas kinetic parameters of linear compressor,” *Measurement*, Vol.125 (2018), pp. 545-553.

10. Li, C. Z., Li, J.G., Sun, J., et al., “Frequency characteristics and Piston Migration characteristics of oil-free linear Compressor,” *Vibration and Shock*, (2019).

11. Sun, J., Li, C., Li, J., et al., “Experimental and Theoretical Investigation of Nonlinear Dynamic characteristics in an Oil-free Moving Coil Linear Compressor,” *2019 7th International Conference on Mechanical Engineering, Materials Science and Civil Engineering*, ICMEMSCE 2019, (2020).